Nuclear Instruments and Methods in Physics Research A 798 (2015) 107–110

Contents lists available at ScienceDirect

Nuclear Instruments and Methods in Physics Research A

journal homepage: www.elsevier.com/locate/nima

A simple method to increase the current range of the TERA chip in charged particle therapy applications

R. Cirio [a,b], F. Fausti [a,c], L. Fanola Guarachi [a,b], S. Giordanengo [a,*], F. Marchetto [a], G. Mazza [a], V. Monaco [a,b], R. Sacchi [a,b], E. Talpacci [b], M. Varasteh Anvar [a,b], A. Vignati [a]

[a] Istituto Nazionale di Fisica Nucleare, sez. di Torino, via P. Giuria,1, 10125 Torino, Italy
[b] Dipartimento di Fisica dell'Università di Torino, via P. Giuria,1, 10125 Torino, Italy
[c] Dipartimento di Elettronica e Telecomunicazioni del Politecnico di Torino, Corso Duca degli Abruzzi, 24, 10129 Torino, Italy

ARTICLE INFO

Article history:
Received 12 March 2015
Received in revised form
30 June 2015
Accepted 10 July 2015
Available online 17 July 2015

Keywords:
Radiotherapy
Charged particles
Ionization chambers
Electronics read-out

ABSTRACT

The development of the next generation of accelerators for charged particle radiotherapy aims to reduce dimensions and operational complexity of the machines by engineering pulsed beams accelerators. The drawback is the increased difficulty to monitor the beam delivery. Within each pulse, instantaneous currents larger by two to three orders of magnitude than present applications are expected, which would saturate the readout of the monitor chambers. In this paper, we report of a simple method to increase by almost two orders of magnitude the current range of an Application Specific Integrated Circuit chip previously developed by our group to read out monitor ionization chambers.

1. Introduction

The technology of the charged particle therapy, also known as hadrontherapy, is rapidly evolving. The main goals of the current developments are the reduction of the accelerating machine dimensions and the possibility of rapidly changing the beam particle energy. The new emerging technologies involve both novel ideas, as laser-driven accelerators [1,2] and cyclinacs [3], and developments of old concepts as synchrocyclotrons [4] and Fixed Field Alternating Gradient accelerators [5]. In most of these, the temporal structure of the beam will deeply change. In current machines the intensity is approximately constant, supplied both in beam spills by synchrotrons (typically a few seconds at most) and all along the delivery time by cyclotrons. In future accelerators short pulses of 1–10 μs duration and a repetition frequency of about 1 kHz are expected, leading to an effective beam duty cycle orders of magnitude smaller than in the present facilities. Thus, to achieve a similar average dose rate, the beam intensity in each pulse will raise accordingly, leading to an increase of difficulty in operating the beam monitor detectors.

In both conventional and charged particle radiotherapy, the precise measurement of the dose delivered to the patient is a very important task that relies on the precision and stability of the measurement systems. Most of the beam monitor detectors are based on ionization chambers [6,7] that offer several advantages in terms of simplicity, robustness and minimal perturbation of the beam. In the perspective of these emerging technologies, the chamber efficiency has to be monitored and eventually corrected for. Additionally, the chamber readout front-end has to cope with expected increase in the input signal.

In this paper we present a simple and effective solution to increase by almost two orders of magnitude the input current range of an Application Specific Integrated Circuit (ASIC) which was designed by our group and used in several laboratories worldwide [6–8], still maintaining a good performance in terms of noise and resolution. The chip, named TERA, implements an architecture based on a charge-to-count converter and integrates 64 equal channels. The performances of the last version of the chip, TERA08, have been thoroughly verified and the results have been published [9].[1]

The current limit of each TERA08 channel is well above the typical currents of few hundreds of nA which are measured in present applications, but is too severe for pulsed accelerators where an instantaneous current during the pulse larger by two to three orders of magnitude is expected. Therefore, one has to increase significantly the current limit redesigning the chip either by increasing the charge per count, at the price of a degraded

* Corresponding author. Tel.: +390116707326.
E-mail address: Simona.Giordanengo@to.infn.it (S. Giordanengo).

[1] The tests published in [9] were performed on the earlier version TERA07 which features only minor differences in the digital part. The results presented thus apply to TERA08 as well.

http://dx.doi.org/10.1016/j.nima.2015.07.013
0168-9002/

charge resolution, or by increasing the count frequency, possibly changing the manufacturing process technology. Both solutions can be effective but require a new circuit implementation.

We propose here a different and simpler solution exploiting the availability of several readout channels in the same chip. It relies on splitting evenly the input current from a detector element into several readout channels and adding up all the counts of these readout channels to reconstruct the input current. We show in this paper that with such an arrangement the input current range is extended proportionally to the number of channels used, and the good linearity observed for each channel individually [9] is preserved. Furthermore, the implementation does not degrade significantly the resolution, being able to measure low currents down to hundreds of pA. As a result, by using all the 64 channels available in the TERA chip, the dynamic range can be increased by almost one order of magnitude.

2. Materials and methods

The TERA08 chip hosts 64 identical channels integrated in a $4.5 \times 5.4\ \text{mm}^2$ die and is designed in the CMOS AMS 0.35 μm technology. In each channel, a conversion from the instantaneous current to a digital pulse frequency is performed, where each digital pulse corresponds to a fixed input charge quantum. The maximum conversion frequency is 20 MHz and the charge quantum can be selected in a range extending up to 1.115 pC; even configuring the charge quantum to this value, the maximum current that a channel can convert before saturation is about 20 μA.

The converter has been designed to accept inputs of both polarities and is followed by a 32 bit counter with up/down counting capability. In this way, both negative (positive) charges can be measured by determining the increment (decrement) of the counter in a given time interval. The operation principle can thus be represented both as a charge-to-pulse-count and as a current-to-pulse-frequency converter.

The converter of each channel is based on the recycling integrator principle and is represented in Fig. 1.

The current I_{in} is integrated over a 600 fF capacitor C_{int} via an operational transconductance amplifier (OTA), where the output voltage is compared to a positive and to a negative threshold by the two synchronous comparators, CMP_1 and CMP_2. Whenever this voltage crosses one of the thresholds the Pulse Generator (PG) sends a pulse to increment or decrement the counter CNT depending on which comparator level was crossed. In parallel, PG sends a pulse to a charge subtraction circuit that subtracts a positive or negative charge quantum to the capacitor C_{int}.

For the measurements presented in this paper, the gain was fixed to a charge quantum of 200 fC, a setting commonly used in clinical applications [8]. It was shown [9] that this gain is fairly uniform across the channels, with a channel-to-channel variation of 1.28% rms.

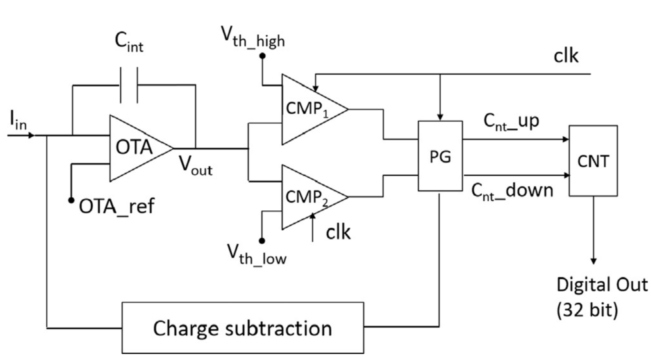

Fig. 1. Schematic of a channel of TERA08.

It was found that the direct connection of two or more Operational Amplifier inputs causes the misbehavior of some of the channels involved. In fact the connection forces the equalization of the input voltages. Differences between the voltage offsets $V_{\text{off}}(\text{i})$ of the input stages, combined with the OTA high gain (~90 dB), would bring most of them in saturation. However, if high value resistors are connected between the channels inputs and the common input node, the channels can work properly as long as the input current is significantly larger than the offset currents needed to keep each OTA input at its correct voltage OTA_ref+V_{off} (i). Montecarlo simulations, performed with the Cadence Specter simulator [10], have shown an average input offset voltage of 0.281 mV, with a sigma of 1.763 mV. A resistor value of 10 MΩ will thus result in a maximum offset current of ±0.26 nA in the ±3 sigma offset range. This value can be considered negligible for our application. It should be noted that the 1.763 mV is a conservative value since it includes also chip-to-chip and wafer-to-wafer variations, while in our case only the offset variations in the same chip are relevant.

Referring to Fig. 2, a board was prepared allowing to split the input into several channels, up to 64, each with its own input resistor. To mimic the detector, an input current I_{in} was fed into the chip. For the measurement of the linearity, a Keithley 2400 [11], operated as a current source, was used. A small ripple was observed in the current produced by this instrument; for the determination of the rms of the measurements, a more stable current provided by a battery was fed.

The readout of the individual channels was performed with a NI FlexRIO FPGA module DAQ module [12] and the data acquisition was developed with the LabView software [13].

3. Results

The chip design has been mainly optimized for low noise and good linearity. After the rearrangement of the inputs, described in the previous section, the measurements were addressed to verify these two features.

3.1. Noise

Two sources contribute to the noise: the pickup at the inputs, where an increase is expected due to the extra-components that have been added, and the noise induced by the background current, offset current included, which adds in each channel to the input current.

To study the background current, we determined the average value of the number of counts and the corresponding spread integrating over an acquisition time interval of 1 ms, i.e. at a readout frequency of 1 kHz. The measurements were performed as a function of the number N of channels connected to the common input, while the input itself was left unconnected. For each of the measurements, the counts of the channels were added. The average number of counts as a function of N is shown in Fig. 3, where each count corresponds to a charge quantum of 200 fC. A linear increase of the background current as a function of N is observed, reaching about 360 pA for $N=64$.

In Fig. 4, we show the rms of the number of counts as a function of N. For a single channel the spread is approximately 0.5 counts, corresponding to 100 fC of charge, and increases as a function of N up to approximately 3.0 counts (i.e. 600 fC) for $N=64$. In terms of current, these uncertainties correspond to 100 pA and 600 pA respectively and are representative of the minimum input current which can be measured at a frequency of 1 kHz. The behavior of the rms is well described by a power function $a \cdot N^b + c$. A χ^2 fit yields $a = (0.12 \pm 0.03)$, $b = (0.73 \pm 0.05)$

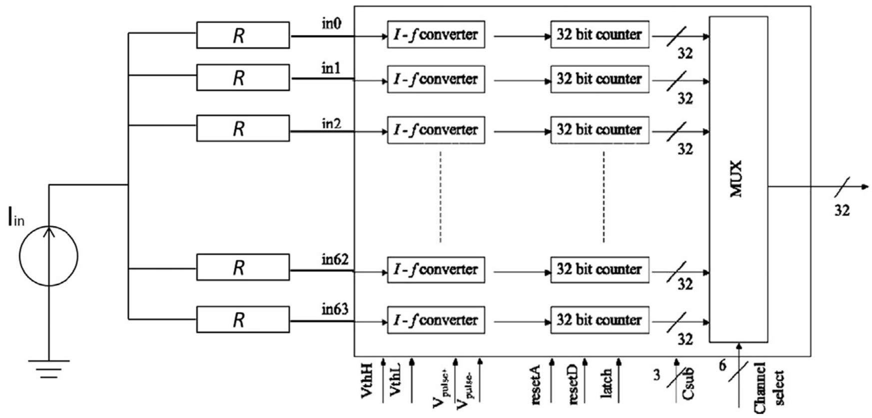

Fig. 2. Setup for the measurements.

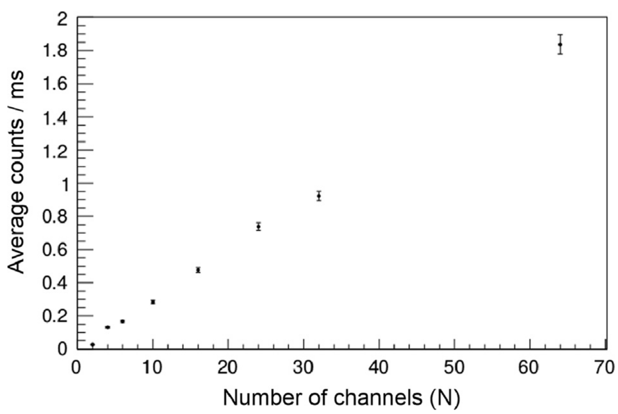

Fig. 3. Average background current in units of counts/ms as a function of the connected number of channels, where the input was left floating. The acquisition time interval was 1 ms.

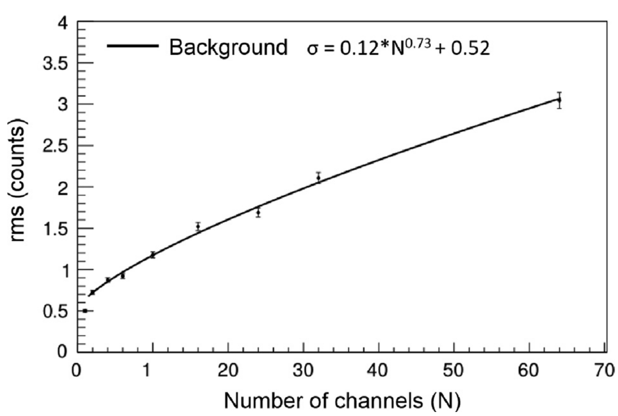

Fig. 4. Rms of the number of counts for the background as a function of the number of channels. Data are fitted with a power function.

and $c = (0.52 \pm 0.05)$. Similar average background current and rms of number of counts were found at smaller readout frequencies, down to few Hz, indicating that the random noise described above is mainly at a much higher frequency than the readout frequency. Consequently, a better sensitivity at very small input currents can be achieved if the readout frequency is reduced.

The rms of the number of counts as a function of the number of channels was also studied with the common input connected through a 10 MΩ resistor to a battery providing a fixed input voltage of 162 V, and the result is shown as the full dots in Fig. 5. It

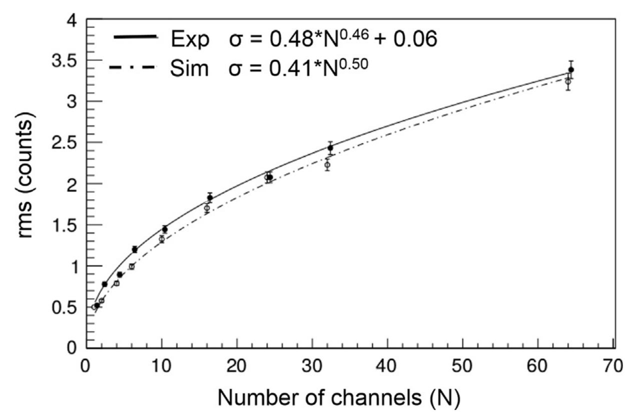

Fig. 5. Rms of the number of counts for a fixed input voltage as a function of the number of channels, where the full dots are the measurements and the open dots are the predictions of the simulation. Both samples are fitted with power functions. For a better comparison, experimental dots are displaced horizontally by a minimum amount to avoid overlaps.

should be noted that the input impedance decreases with the increase of the number of channels N connected to the input, therefore each point corresponds to a different input current I_{in} ranging from 75 nA ($N=1$) to 158 nA ($N=64$).

Again, a fit to the power function $a \cdot N^b + c$ yields $a = (0.48 \pm 0.07)$, $b = (0.46 \pm 0.03)$ and $c = (0.06 \pm 0.07)$. This result indicates that the dominant contribution to the uncertainty of each channel is the sensitivity of its counter, contributing with an rms of approximately $\pm$ 0.5 counts, and that the channels are behaving as identical uncorrelated counters, which explains the $N^{0.5}$ behavior. This interpretation is confirmed by a simulation based on a simple model where the channels are described as non-correlated counters, the only correlation being the charge conservation, i.e. the sum of the currents integrated in each channel should preserving the total input charge. The input impedances and the gains of the channel are assumed to randomly vary between channels by $\pm$ 2% and $\pm$ 1% respectively, and the initial charge integrated in the C_{int} capacitor of each channel is sampled with uniform probability between 0 the charge quantum of 200 fC. The predictions of the model are shown as open dots in Fig. 5. A good agreement with the measurements is observed, the fit to the same power function yielding $a = (0.41 \pm 0.01)$, $b = (0.50 \pm 0.01)$ and $c = (0.00 \pm 0.06)$.

3.2. Linearity

The linearity was studied by injecting a steady current and by measuring the average number of counts over an acquisition time

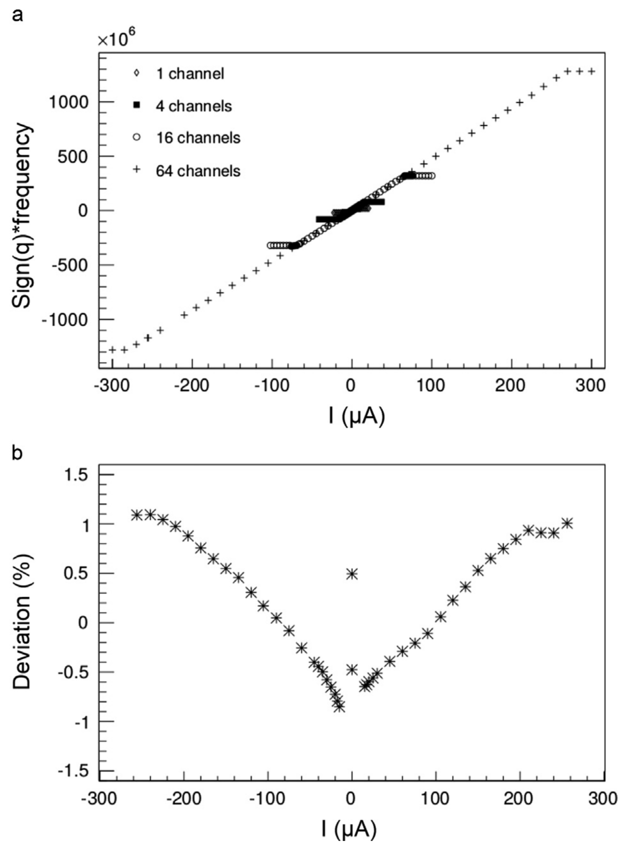

Fig. 6. a. Output frequency vs. input current as a function of the number of channels; 6b. Relative deviation from linearity.

interval of 1 ms. The results are presented in Fig. 6a, where we show the output pulse frequency as a function of the input current. Linearity of the output is achieved in a current range which increases proportionally to the number of channel N, reaching a maximum of ± 256 μA for $N=64$. The data with $N=64$ were fitted to a straight line, for positive and negative input currents separately, in the range $\pm$(5 nA–256 μA) and the relative deviations are shown in Fig. 6b. The deviations from linearity are found to be within $\pm 1\%$, which is considered acceptable in most of the radiotherapy applications, while for currents smaller than 5 nA, where the input current becomes comparable to the offset currents, the deviations tend to diverge. We remark that this interval corresponds to a dynamic range of $\sim 5 \times 10^4$, a 5-fold increase compared to a single channel as reported in [9].

4. Conclusions

Evolvements of the accelerators for radiotherapeutic treatments with charged particles call for an increase of the accepted input current of the front-end electronics. In this paper, we present a simple method for the TERA chip to gain almost two orders of magnitude in the input current range. The increase in the rms of the measurements is limited and the linearity over the increased range is still within 1%, which is considered acceptable in this field. The resulting dynamic range is also considerably increased.

References

[1] M. Dunne, Science 312 (5772) (2006) 374. http://dx.doi.org/10.1126/science.1126051, and references therein.
[2] G.A.P. Cirrone, et al., Proceedings of SPIE 8779 (63) (2013), http://dx.doi.org/10.1117/12.2026530, and references therein.
[3] U. Amaldi, et al., Nuclear Instruments and Methods in Physics Research Section A 620 (2010) 563.
[4] W. Kleeven et al.. "The IBA superconducting synchrocyclotron project S2C2", in: Proceedings of Cyclotrons'13 (20th International Conference on Cyclotrons and Their Applications), Vancouver, Canada, September 16–20 2013.
[5] B. Qin, Y. Mori, Nuclear Instruments and Methods in Physics Research Section A 648 (2011) 28.
[6] N. Givehchi, et al., Nuclear Instruments and Methods in Physics Research Section A 572 (2007) 1094.
[7] A. La Rosa, et al., Nuclear Instruments and Methods in Physics Research Section A 565 (2006) 833.
[8] S. Giordanengo, et al., Nuclear Instruments and Methods in Physics Research Section A 698 (2013) 202.
[9] A. La Rosa, et al., Nuclear Instruments and Methods in Physics Research Section A 583 (2007) 461.
[10] 〈http://www.cadence.com/products/cic/spectre_circuit/pages/default.aspx〉.
[11] 〈http://www.keithley.com/knowledgecenter/knowledgecenter_pdf/2400_902_01D.pdf〉.
[12] 〈http://www.ni.com/pdf/manuals/373047b.pdf〉.
[13] 〈http://www.ni.com/labview/〉.